J|A|C|S
ARTICLES
Published on Web 09/28/2002

Polyferrocenylsilane Microspheres: Synthesis, Mechanism of Formation, Size and Charge Tunability, Electrostatic Self-Assembly, and Pyrolysis to Spherical Magnetic Ceramic Particles

Kevin Kulbaba,[†] Alison Cheng,[†] Alexandra Bartole,[†] Sharonna Greenberg,[†] Rui Resendes,[†] Neil Coombs,[†] Athena Safa-Sefat,[‡] John E. Greedan,[‡] Harald D. H. Stöver,*[,‡] Geoffrey A. Ozin,*[,†] and Ian Manners*[,†]

Contribution from the Department of Chemistry, University of Toronto, Toronto, Ontario, Canada M5S 3H6, and Department of Chemistry, McMaster University, Hamilton, Ontario, Canada L8S 4M1

Received February 11, 2002

Abstract: Pt(0)-catalyzed ring-opening precipitation copolymerization of [1]silaferrocenophanes $fcSiMe_2$ (**3**) and the spirocyclic cross-linker $fcSi(CH_2)_3$ (**4**) (fc = $Fe(\eta^5\text{-}C_5H_4)_2$) was used to prepare polyferrocenylsilane microspheres (PFSMSs) under mild conditions. By varying the reaction conditions, a wide variety of other morphologies was obtained. The effects of temperature, monomer ratio, solvent composition, catalyst concentration, and time on the observed morphology were investigated and interpreted in terms of a mechanism for microsphere formation. The most well-defined particles were formed using equimolar amounts of **3** and **4**, in a 50:50 mixture of xylenes and decane at 60 °C with gentle agitation. Chemical oxidation of the polymeric microspheres led to positively charged particles (OPFSMSs) which underwent electrostatically driven self-assembly with negatively charged silica microspheres to form core−corona composite particles. Redox titration with controlled amounts of the one-electron oxidant $[N(C_6H_4Br\text{-}p)_3][PF_6]$ in acetonitrile led to the oxidation of the outer 0.15 μm (ca. 32%) of the PFSMSs. The resulting OPFSMSs were reduced back to their neutral form by reaction with hydrazine in methanol. Pyrolysis of the PFSMSs led to spherical magnetic ceramic replicas with tunable magnetic properties that organize into ordered 2-D arrays at the air−water interface under the influence of a magnetic field.

Introduction

Spherical, colloidal particles are of intense interest with respect to applications in catalysis and separation science and as chemical sensors.[1−5] Silica particles have been used to construct highly ordered structures termed colloidal crystals, which are ideal for photonic applications.[5] Relatively small changes in the periodicity or ordering within these crystals will elicit an optical response, making them useful in sensing applications. For example, Asher and co-workers have developed a hydrophilic polymeric colloidal crystalline array with the ability to sense changes in pH and ionic strength within aqueous solutions by measuring the optical Bragg diffraction peak of the material.[2] Highly ordered, porous structures have also been formed from a variety of organic and inorganic materials using colloidal crystal templates.[6]

The surface properties of spherical colloidal particles can be tailored by coating with or encapsulation in a desired material.[3] The ability to tailor the surface characteristics in a controlled and specific manner while maintaining particle stability allows access to highly specialized sensors, biocatalysts, and drug delivery systems.[4] However, the formation of such functional

* Address correspondence to these authors. E-mail: gozin@chem.utoronto.ca (G.A.O.); imanners@chem.utoronto.ca (I.M.); stoverh@mcmaster.ca (H.D.H.S.).
[†] University of Toronto.
[‡] McMaster University.

(1) See for example: (a) Barrett, A. G. M.; de Miguel, Y. R. *Chem. Commun.* **1998**, 2079. (b) Roscoe, S. B.; Fréchet, J. M. J.; Walzer, J. F.; Dias, A. J. *Science* **1998**, *280*, 270. (c) Li, W.-H.; Stöver, H. D. H.; Hamielec, A. E. *J. Polym. Sci., Part A: Polym. Chem.* **1994**, *32*, 2029. (d) Holtz, J. H.; Asher, S. A. *Nature* **1997**, *389*, 829. (e) Goodey, A.; Lavigne, J. J.; Savoy, S. M.; Rodriguez, M. D.; Curey, T.; Tsao, A.; Simmons, G.; Wright, J.; Yoo, S.-J.; Sohn, Y.; Anslyn, E. V.; Shear, J. B.; Neikirk, D. P.; McDevitt, J. T. *J. Am. Chem. Soc.* **2001**, *123*, 2559. (f) Xia, Y.; Gates, B.; Yin, Y.; Lu, Y. *Adv. Mater.* **2000**, *12*, 693.
(2) (a) Weissman, J. M.; Sunkara, H. B.; Tse, A. S.; Asher, S. A. *Science* **1996**, *274*, 959. (b) Lee, K.; Asher, S. A. *J. Am. Chem. Soc.* **2000**, *122*, 9534.
(3) (a) Caruso, F. *Adv. Mater.* **2001**, *13*, 11. (b) Ji, T.; Lirtsman, V. G.; Avny, Y.; Davidov, D. *Adv. Mater.* **2001**, *13*, 1253.
(4) (a) Velev, O. D.; Kaler, E. W. *Langmuir* **1999**, *15*, 3693. (b) Dokoutchaev, A.; James, J. T.; Koene, S. C.; Pathak, S.; Prakash, G. K. S.; Thompson, M. E. *Chem. Mater.* **1999**, *11*, 2389. (c) Loxley, A.; Vincent, B. *J. Colloid Interface Sci.* **1998**, *208*, 49. (d) Yin, Y.; Lu, Y.; Gates, B.; Xia, Y. *Chem. Mater.* **2001**, *13*, 1146.
(5) (a) Yablonovitch, E. *J. Phys.: Condens. Matter* **1993**, *5*, 2443. (b) Ni, P.; Dong, P.; Cheng, B.; Li, X.; Zhang, D. *Adv. Mater.* **2001**, *13*, 437. (c) Miguez, H.; Meseguer, F.; López, C.; López-Tejeira, F.; Sánchez-Dehesa, J. *Adv. Mater.* **2001**, *13*, 393. (d) Joannopoulos, J. D.; Meade, R. D., Ed.; Winn, J. N., Ed. *Photonic Crystals: Molding the Flow of Light*; Princeton University Press: Toronto, 1995.
(6) (a) Kulinowski, K. M.; Jiang, P.; Vaswani, H.; Colvin, V. L. *Adv. Mater.* **2000**, *12*, 833. (b) Velev, O. D.; Kaler, E. W. *Adv. Mater.* **2000**, *12*, 531. (c) Johnson, S. A.; Ollivier, P. J.; Mallouk, T. E. *Science* **1999**, *283*, 963. (d) Holland, B. T.; Blanford, C. F.; Do, T.; Stein, A. *Chem. Mater.* **1999**, *11*, 795. (e) Blanco, A.; Chomski, E.; Grabtchak, S.; Ibisate, M.; John, S.; Leonard, S. W.; Lopez, C.; Meseguer, F.; Miguez, H.; Mondia, J. P.; Ozin, G. A.; Toader, O.; van Driel, H. M. *Nature* **2000**, *405*, 437.

10.1021/ja0202053 CCC: $22.00

materials requires postmodification steps that can be both time-consuming and incomplete.

At present, polymer microsphere technology has been limited to systems based on organic polymers, which are generally relatively inert. The development of microspheres based on metal-containing polymers exhibiting interesting redox, semiconductive, and preceramic properties innate to the polymer may prove useful in the evolution of highly specialized, functional materials.[3−8] Polyferrocenylsilanes (PFSs) **2** represent a recently established, readily accessible class of metallopolymers with a main chain consisting of alternating ferrocene and organosilane units.[9,10] High molecular weight samples of these materials were first prepared in the early 1990s by thermal ring-opening polymerization (ROP) of silicon-bridged [1]silaferrocenophanes (**1**). This chain growth synthetic approach permitted access to very high molecular weight polymers **2** with average molecular

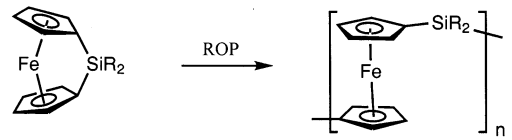

1 **2**

weights on the order of $M_w = 10^5-10^6$ and $M_n > 10^5$. This ROP methodology has been expanded to a range of analogous strained monomers which contain other bridging elements (germanium, tin, phosphorus, sulfur, etc.) and transition metals or different π-hydrocarbon rings.[11] More recently living anionic and transition-metal-catalyzed routes have also been established, permitting unprecedented control of organometallic polymer architectures.[12,13]

Due to the redox-active ferrocene units present in the polymer main chain, these materials possess interesting physical and chemical properties.[10,14] For example, cyclic voltammetric studies of **2** have revealed the presence of Fe···Fe interactions along the polymer backbone, and when oxidatively doped, these materials become p-type semiconductors with hole conductivities up to ca. 10^{-4} S·cm^{-1}.[10,15] As a result, polyferrocenylsilanes have been investigated for use as charge dissipation coatings

Scheme 1

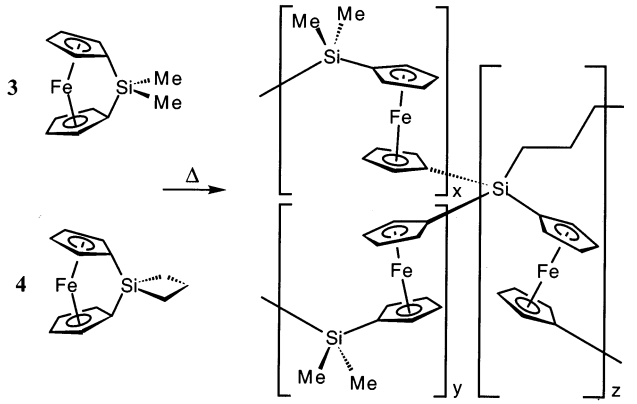

5

for dielectrics,[16] in the formation of redox-active gels (Scheme 1),[17,18] and as components of superlattices formed from layer-by-layer self-assembly.[19,20] Recently, we have shown that the cross-linked matrix **5** ($x = y = 0$), obtained from the thermal ROP of the spirocyclic cross-linker **4** (Scheme 1), forms well-defined ceramics containing α-Fe nanoclusters within an amorphous "carbosilane" matrix when pyrolyzed at 600−1000 °C.[21] The magnetic properties of these bulk ceramics could be tuned within this temperature range. More specifically, at temperatures of 600−850 °C, small, single-domain superparamagnetic α-Fe nanoparticles are formed, while, at 1000 °C, larger ferromagnetic, multidomain α-Fe nanoparticles are generated. Hyperbranched ferrocenylsilane polymers have recently been shown to possess interesting preceramic properties.[22] Such cross-linked networks produce magnetic, electrically conductive, macroporous ceramics with interconnected nanoclusters at 1000−1200 °C.

Herein we report the full details of our work in the synthesis of microspheres comprised of PFSs, which possess interesting redox and preceramic properties innate to the particles which do not require further postmodification steps.[23]

(7) See for example: (a) Manners, I. *Angew. Chem., Int. Ed. Engl.* **1996**, *35*, 1602. (b) Kingsborough, R. P.; Swager, T. M. *Prog. Inorg. Chem.* **1999**, *48*, 123. (c) Nguyen, P.; Gómez-Elipe, P.; Manners, I. *Chem. Rev.* **1999**, *99*, 1515. (d) Archer, R. D. *Inorganic and Organometallic Polymers*; John Wiley & Sons: New York, 2001. (e) Manners, I. *Science* **2001**, *294*, 1664.
(8) (a) Caruso, F.; Susha, A. S.; Giersig, M.; Möhwald, H. *Adv. Mater.* **1999**, *11*, 950. (b) Winnik, F. M.; Morneau, A.; Ziolo, R. F.; Stöver, H. D. H.; Li, W.-H. *Langmuir* **1995**, *11*, 3660. (c) Burke, N. A. D.; Stöver, H. D. H.; Dawson, F. P.; Lavers, J. D.; Jain, P. K.; Oka, H. *IEEE Trans. Magn.* **2001**, *37*, 2660. (d) Khan, M. A.; Armes, S. P. *Adv. Mater.* **2000**, *12*, 671. (e) Wiersma, A. E.; vd Steeg, L. M. A.; Jongeling, T. J. M. *Synth. Met.* **1995**, *71*, 2269.
(9) Foucher, D. A.; Tang, B. Z.; Manners, I. *J. Am. Chem. Soc.* **1992**, *114*, 6246.
(10) Review: Kulbaba, K.; Manners, I. *Macromol. Rapid Commun.* **2001**, *22*, 711.
(11) (a) Manners, I. *Can. J. Chem.* **1998**, *76*, 371. (b) Resendes, R.; Nelson, J. M.; Fischer, A.; Jäkle, F.; Bartole, A.; Lough, A. J.; Manners, I. *J. Am. Chem. Soc.* **2001**, *123*, 2116.
(12) (a) Rulkens, R.; Lough, A. J.; Manners, I. *J. Am. Chem. Soc.* **1994**, *116*, 797. (b) Ni, Y.; Rulkens, R.; Manners, I. *J. Am. Chem. Soc.* **1996**, *118*, 4102.
(13) (a) Ni, Y.; Rulkens, R.; Pudelski, J. K.; Manners, I. *Macromol. Rapid Commun.* **1995**, *16*, 637. (b) Reddy, N. P.; Yamashita, H.; Tanaka, M. *J. Chem. Soc., Chem. Commun.* **1995**, 2263. (c) Gómez-Elipe, P.; Resendes, R.; Macdonald, P. M.; Manners, I. *J. Am. Chem. Soc.* **1998**, *120*, 8348.
(14) (a) Barlow, S.; Rohl, A. L.; Shi, S.; Freeman, C. M.; O'Hare, D. *J. Am. Chem. Soc.* **1996**, *118*, 7578. (b) Papkov, V. S.; Gerasimov, M. V.; Dubovik, I. I.; Sharma, S.; Dementiev, V. V.; Pannell, K. H. *Macromolecules* **2000**, *33*, 7107. (c) Chen, Z.; Foster, M. D.; Zhuo, W.; Fong, H.; Reneker, D. H.; Resendes, R., Manners, I. *Macromolecules* **2001**, *34*, 6156.
(15) (a) Rulkens, R.; Lough, A. J.; Manners, I.; Lovelace, S. R.; Grant, C.; Geiger, W. E. *J. Am. Chem. Soc.* **1996**, *118*, 12683. (b) Foucher, D. A.; Honeyman, C. H.; Nelson, J. M.; Tang, B. Z.; Manners, I. *Angew. Chem., Int. Ed. Engl.* **1993**, *32*, 1709. (c) Espada, L.; Pannell, K. H.; Papkov, V.; Leites, L.; Bukalov, S.; Suzdalev, I.; Tanaka, M.; Hayashi, T. *Organometallics* **2002**, *21*, 3758.
(16) Resendes, R.; Berenbaum, A.; Stojevic, G.; Jäkle, F.; Bartole, A.; Zamanian, F.; Dubois, G.; Hersom, C.; Balmain, K.; Manners, I. *Adv. Mater.* **2000**, *12*, 327.
(17) (a) MacLachlan, M. J.; Lough, A. J.; Manners, I. *Macromolecules* **1996**, *29*, 8562. (b) Kulbaba, K.; MacLachlan, M. J.; Evans, C. E. B.; Manners, I. *Macromol. Chem. Phys.* **2001**, *202*, 1768.
(18) Calléja, G.; Cerveau, G.; Corriu, R. J. P. *J. Organomet. Chem.* **2001**, *621*, 46.
(19) (a) Ginzburg, M.; Galloro, J.; Jäkle, F.; Power-Billard, K. N.; Yang, S.; Sokolov, I.; Lam, C. N. C.; Neumann, A. W.; Manners, I.; Ozin, G. A. *Langmuir* **2000**, *16*, 9609. (b) Hempenius, M. A.; Robins, N. S.; Lammertink, R. G. H.; Vancso, G. J. *Macromol. Rapid Commun.* **2001**, *22*, 30.
(20) Polyferrocenylsilanes have also attracted attention as variable refractive index materials and etching resists. (a) Espada, L. I.; Shadaram, M.; Robillard, J.; Pannell, K. H. *J. Inorg. Organomet. Polym.* **2001**, *10*, 169. (b) Cheng, J. Y.; Ross, C. A.; Chan, V. Z.-H.; Thomas, E. L.; Lammertink, R. G. H.; Vancso, G. J. *Adv. Mater.* **2001**, *13*, 1174. (c) Massey, J. A.; Winnik, M. A.; Manners, I.; Chan, V. Z.-H.; Ostermann, J. M.; Enchelmaier, R.; Spatz, J. P.; Möller, M. *J. Am. Chem. Soc.* **2001**, *123*, 3147.
(21) (a) MacLachlan, M. J.; Ginzburg, M.; Coombs, N.; Coyle, T. W.; Raju, N. P.; Greedan, J. E.; Ozin, G. A.; Manners, I. *Science* **2000,** *287*, 1460. (b) Ginzburg, M.; MacLachlan, M. J.; Yang, S. M.; Coombs, N.; Coyle, T. W.; Raju, N. P.; Greedan, J. E.; Herber, R. H.; Ozin, G. A.; Manners, I. *J. Am. Chem. Soc.* **2002**, *124*, 2625.
(22) Sun, Q.; Lam, J. W. Y.; Xu, K.; Xu, H.; Cha, J. A. K.; Wong, P. C. L.; Wen, G.; Zhang, X.; Jing, X.; Wang, F.; Tang, B. Z. *Chem. Mater.* **2000**, *12*, 2617.

Results and Discussion

Heterogeneous polymerization is currently the most commonly employed synthetic technique for the formation of monodisperse polymer microspheres. In general, these processes require the addition of electrostatic or steric stabilizers (e.g., sodium lauryl sulfate, $CH_3(CH_2)_{11}OSO_3^-Na^+$, or poly(vinyl alcohol)) to a suspension of monomer in a nonsolvent with constant, vigorous stirring.[24] Such techniques generate uniform particles ranging in size from ca. 50 nm up to several micrometers in diameter. Templating agents have been added to the polymerization mixtures to afford molecularly imprinted microspheres which display selective binding efficiencies and have been successfully used for the separation of chiral pharmaceutical compounds.[25] Such methods however are not straightforward and may use special dispersing phases, functional surfactant, and multistep swelling operations in intermediate media. Additional purification steps become necessary as residual stabilizer molecules incorporated within the polymer spheres may adversely affect the properties of the resulting particles.

This inherent drawback is not found with precipitation polymerization methodologies, which, under appropriate conditions, can generate polymer microspheres of tunable size and porosity without the use of additional stabilizers.[26] These controlled precipitation polymerizations begin with a homogeneous mixture of monomer, initiator, and solvent. During the polymerization, the polymer may phase-separate from solution due to enthalpic factors (due to poor polymer−solvent interactions) or entropic effects arising from the cross-linking of the polymer network, which prevents the polymer and solvent from freely mixing. In good solvents such polymerizations produce turbid macroscopic or microscopic gels, depending on the original monomer concentration and relative amount of cross-linking of the polymer network. In poorer solvents, precipitation polymerizations normally produce micrometer-sized particles; however, the size distribution is often broad due to a lack of colloidal stability.

In 1993, Li and Stöver reported the synthesis of monodisperse crosslinked microspheres through a one-step, stabilizer-free, AIBN (2,2′-azobis(isobutyronitrile))-initiated precipitation polymerization of DVB-55 (a mixture of 55% *m*- and *p*-divinylbenzene and 45% *m*- and *p*-ethylvinylbenzene) in acetonitrile.[26a] Such a system provides a reasonable polymerization rate and at low concentrations of monomer allows for controlled growth of discrete particles. The mechanism of particle formation has been investigated in detail and is believed to occur by a two-step process involving particle nucleation and then growth (see Scheme 2).[27] Aggregation and subsequent cross-linking of soluble oligomers produces solvent-swollen

Scheme 2

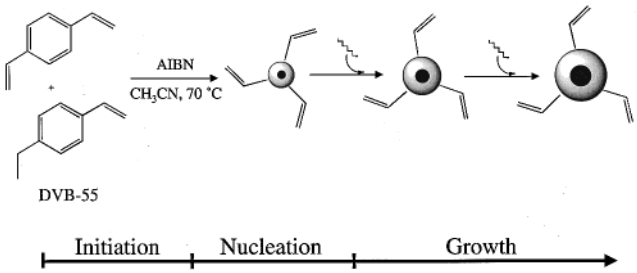

microgels which subsequently desolvate to form particle nuclei. Larger particles are formed by capture of soluble oligomeric radicals from solution by reactive vinyl groups on the particle surface. Thus, as the polymerization proceeds in marginal, near-Θ solvents (such as acetonitrile, or mixtures of methyl ethyl ketone and heptane), this transient gel layer continuously desolvates and collapses, while newly formed oligomer molecules are bonded to the surface. It is believed that this solvent-swollen outer gel layer sterically stabilizes the particles, preventing coagulation that would otherwise lead to a broad size distribution. This autosteric stabilization allows for the formation of polymer microspheres in a variety of near-Θ solvents. Furthermore, by varying the solvents used and the concentration of monomers in solution, the porosity and the size of the resulting particles can be controlled.[26b]

Gentle rotation of the reaction vessel serves to maintain a suspension of growing particles and effectively reduces the interparticle contact time, preventing aggregation of the growing particles and allowing for uniform growth.

Synthesis of Polyferrocenylsilane Microspheres (PFSMSs). (i) Initial Considerations. Given the mild reaction conditions under which polystyrene particles can be prepared and the ease with which the size and morphology can be varied, it is desirable to extend this precipitation polymerization methodology toward the synthesis of cross-linked microspheres derived from other polymers. If such a method is to be employed to form PFSMSs, certain criteria must be met. The precatalyst should be homogeneous in nature and allow for a significant degree of cross-linking of the particles. The solvency of the continuous phase must be chosen to provide the necessary near-Θ solvent−polymer interactions that allow for controlled precipitation of the polymer particles. Monomer concentrations should also be kept near those required for polystyrene microspheres (2−5 vol % DVB-55) under appropriate reaction conditions.[27]

Homogeneous precatalysts such as Karstedt's catalyst (a divinyltetramethyldisiloxane−Pt(0) complex) are known to catalyze the ROP of the [1]silaferrocenophane **3**, as well as the spirocyclic [1]silaferrocenophane cross-linker **4**.[28,29] As polymer−solvent interactions play a key role in the formation of autostabilized microspheres, it was necessary to choose a system for which the solvency could be tuned over a wide range. Mixtures of xylenes and decane were utilized as they are miscible in all proportions and xylenes are considered to be a good solvent for **2** while decane is known to function as a precipitant. Thus, an extension of the precipitation polymeri-

(23) Communication: Kulbaba, K.; Resendes, R.; Cheng, A.; Bartole, A.; Safa-Sefat, A.; Coombs, N.; Stöver, H. D. H.; Greedan, J. E.; Ozin, G. A.; Manners, I. *Adv. Mater.* **2001**, *13*, 732.

(24) (a) Napper, D. H. *Polymeric Stabilization of Colloidal Dispersions*; Academic Press: London, 1983. (b) Bassett, D. R.; Hoy, K. L. *Polymer Colloids*, 2nd ed.; Plenum Press: New York, 1980. (c) *Polymer Latexes: Preparation, Characterization, and Applications*; Daniels, E. S., Sudol, E. D., El-Aasser, M. S., Eds.; ACS Symposium Series 492; American Chemical Society: Washington, DC, 1992; p 12.

(25) (a) Mayes, A. G.; Mosbach, K. *Anal. Chem.* **1996**, *68*, 3769. (b) Lei, Y.; Weiss, R.; Mosbach, K. *Macromolecules* **2000,** *33*, 8239.

(26) (a) Li, K.; Stöver, H. D. H. *J. Polym. Sci., Part A: Polym. Chem.* **1993**, *31*, 3257. (b) Li, W.-H.; Stöver, H. D. H. *J. Polym. Sci., Part A: Polym. Chem.* **1998**, *36*, 1543.

(27) (a) Downey, J. S.; McIsaac, G.; Frank, R. S.; Stöver, H. D. H. *Macromolecules* **2001**, *34*, 4534. (b) Downey, J. S.; Frank, R. S.; Li, W.-H.; Stöver, H. D. H. *Macromolecules* **1999**, *32*, 2838.

(28) (a) Cundy, C. S.; Eaborn, C.; Lappert, M. F. *J. Organomet. Chem.* **1972**, *44*, 291. (b) Koopmann, F.; Frey, H. *Macromolecules* **1996**, *29*, 3701.

(29) Temple, K.; Jäkle, F.; Sheridan, J. B.; Manners, I. *J. Am. Chem. Soc.* **2001**, *123*, 1355.

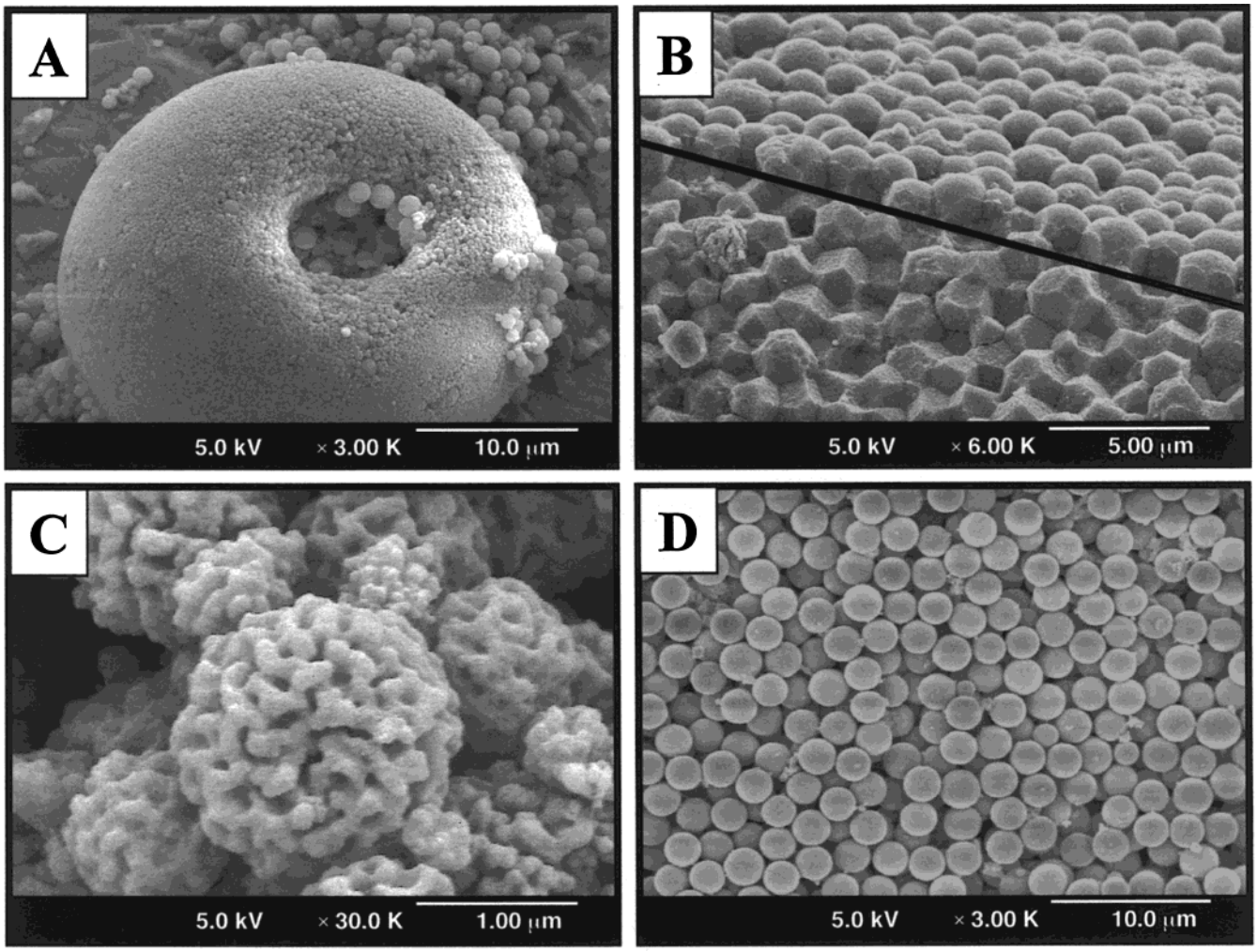

Figure 1. Some interesting morphologies of PFS particles. Synthesis of PFSMSs without the gentle agitation tends to produce irregular morphologies. The samples were prepared at identical concentrations without (A−C) and with (D) mechanical agitation by rolling the reaction vessel on its long axis.

zation methodology developed by Stöver's group to the synthesis of PFSMSs through a transition-metal-catalyzed route seemed feasible.

(ii) Preparation of PFSMSs via Precipitation Polymerization. To probe the effect of solvent interactions on particle formation, a range of solvent mixtures of xylenes and decane were investigated, with a constant monomer concentration and amount of added catalyst (1.2 mol %) and an equimolar ratio of monomer **3** and cross-linker **4**. A 50:50 mixture of xylenes and decane gave the most promising results. However, at room temperature (25 °C), such precipitation polymerization reactions afford only minor amounts of PFSMSs with a large percentage of morphologically poorly defined, insoluble polymeric material.

With polystyrene systems, a competitive cross-link rate is essential to control particle growth. For the present system, the silacyclobutane ring of the spirocyclic ferrocenophane **4** is known to be less reactive than the strained [1]ferrocenophane ring of **3** and **4**.[30] This difference in reactivity of monomer **4** may cause a reduced cross-linking rate, especially at lower temperatures. By increasing the temperature of the reaction to 60 °C, there is presumably an increase in the cross-link rate since the resulting particles appear more spherical in nature. However, they still possess relatively high polydispersity indices (PDI > 1.5), and several irregular morphologies can also be observed (see Figure 1A−C). Gentle rolling of the reaction vessels on their long axis improved both the quality and the quantity of PFSMSs formed, with the dominant morphology now being smooth, spherical particles of much more uniform size (PDI near 1.1; see Figure 1D).

Previous work has shown that monodisperse polymer microspheres self-assemble into highly ordered monolayers through the use of LB film casting techniques.[31] Given that the PFSMSs are relatively monodisperse, the formation of well-ordered monolayers was investigated. SEM analysis of the resulting film shows a monolayer of PFSMSs (Figure 2A). Upon close inspection regions of hexagonally close-packed spheres become apparent (Figure 2B).

The molecular structure of the PFSMSs was investigated by solid-state NMR spectroscopy.[32−34] The spectra were consistent with a cross-linked material with variable cross-link sites within the polymer network similar to previously studied thermally cross-linked analogues.[17,21]

(30) MacLachlan, M. J.; Ginzburg, M.; Zheng, J.; Knöll, O.; Lough, A. J.; Manners, I. *New J. Chem.* **1998**, 1409.

(31) (a) Hulteen, J. C.; Treichel, D. A.; Smith, M. T.; Duval, M. L.; Jensen, T. R.; Van Duyne, R. P. *J. Phys. Chem. B* **1999**, *103*, 3854. (b) Lenzmann, F.; Li, K.; Kitai, A. H.; Stöver, H. D. H. *Chem. Mater.* **1994**, *6*, 156.

(32) Ginzburg, M.; MacLachlan, M. J.; Yang, S. M.; Coombs, N. Coyle, T. W.; Raju, N. P.; Greedan, J. E.; Herber, R. H.; Ozin, G. A.; Manners, I. *J. Am. Chem. Soc.* **2002**, *124*, 2625.

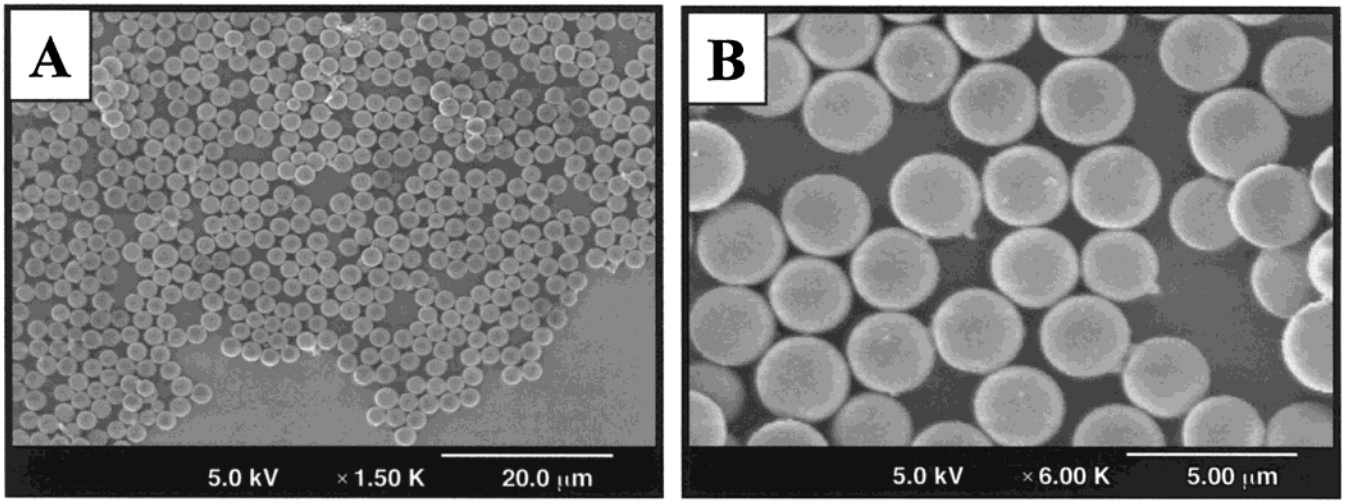

Figure 2. SEM micrographs of (A) a PFSMS monolayer formed by a simple dip-coating technique[31b] and (B) a close-packed region at higher magnification.

Mechanism of Formation of PFSMSs. An increased understanding of the mechanism of formation for these PFSMSs may allow for the generation of optimized particles, with increased control over the resulting particle size, polydispersity, surface morphology, and composition.[33] Particle formation was suspected to occur through an analogous reaction mechanism to that proposed for the crosslinked polystyrene microspheres (Scheme 2). To this end, the effects of solvent composition, monomer ratio, catalyst concentration, and time on the particle morphology were investigated.

(i) Solvent Interactions. To investigate the effects of varying the solvency of the continuous phase, the solvent composition was varied from 100% xylenes to 100% decane while all other parameters were held constant.

(a) Particles Formed in the Collapsed State. At high decane compositions (>75%), the newly formed polymer precipitates from solution and covers the walls of the reaction vessel. Upon workup the resulting material appeared by SEM analysis to be composed primarily of interconnected polymer microspheres ca. 0.7 μm in diameter.[34] Very few discrete particles were observed. Particles formed in such a medium will not possess a significant swollen gel layer. The formation of autostabilized microspheres is not possible in this instance as newly formed particles cannot maintain colloidal stability. In pure decane, the polymeric material coats the walls of the reaction vessel and forms a finely dispersed solid which appears to be soluble in tetrahydrofuran. Analysis of this sample by GPC revealed a bimodal distribution with a low molecular weight fraction with an M_n of 4700 (PDI of 1.8) and a high molecular weight fraction with M_n > 2,000,000 using polystyrene standards. Such high molecular weight species are the result of the cross-linking of reactive oligomers to form microgels or highly branched polymers that appear soluble, or at least dispersible, in THF.

(b) Particles Formed in the Swollen State. At high xylenes compositions (>65%) highly swollen microgels are formed which remain in suspension until centrifugation.[34] When these swollen microgels are dispersed in a non-solvent such as methanol, the nonhomogeneous network collapses to produce discrete particles with a highly variable surface topology. PFSMSs were not produced under these conditions due to the polymer segment−solvent interactions being too favorable, which prevents the necessary collapse of the network to form discrete nucleation sites.

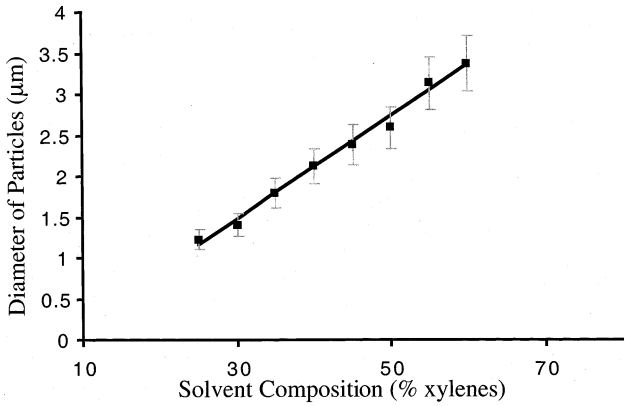

Figure 3. Relationship between the solvency of the reaction medium (percent xylenes in decane) and the diameter of the resulting PFSMSs.

(c) Particles Formed at Near-Θ Conditions. At intermediate solvency (30−60% xylenes) polymer microspheres were observed by SEM to be the dominant morphology with diameters between 1.2 μm (30% xylenes) and 3.5 μm (60% xylenes) with polydispersity indices near 1.1.[34] Therefore, the solvent conditions met the requirements for autostabilized PFSMSs. By analogy with polystyrene microspheres, the growing particles should contain a solvent-swollen outer shell and a collapsed inner core under such conditions. Growth can be assumed to occur by capture of reactive oligomers from solution onto the surface of the particles.

The size of the PFSMSs was observed to increase linearly with increasing xylenes concentration (see Figure 3) in the range between 25% and 60% xylenes in decane (see Table 1).

The most well-defined spheres were produced at solvent compositions near 50% xylenes, with average diameters of 2.6 μm (PDI of 1.10). By performing reactions on larger scales (75

(33) The precipitation polymerization techniques described in this paper have been extended to the synthesis of PFSMSs from fcSiMePh and the spirocyclic cross-linker **4**. The resulting spherical particles had an average diameter of 1.84 μm and a PDI of 1.17 (see the Supporting Information). The fcSiMePh monomer was synthesized according to literature procedures (see ref 29).

(34) See the Supporting Information for solid-state NMR, reflectance UV−vis/near-IR, XPS, and PXRD data as well as SEM and TEM images for PFSMSs formed under these conditions.

Table 1. Effect of Solvent Composition on the Observed Particle Morphology

amt of xylenes (%)	av diam (μm)	PDI	morphology
0	0.3	1.47	soluble polymer
20	0.7	1.34	interconnected particles
25	1.2	1.13	interconnected particles
30	1.4	1.08	spheres
35	1.8	1.10	spheres
40	2.1	1.14	spheres
45	2.4	1.10	spheres
50	2.6	1.10	spheres
55	3.1	1.13	spheres
60	3.4	1.13	spheres
65	1.0	1.43	spheres (bimodal)
	3.2	1.21	spheres (bimodal)
80	0.2	1.52	microgels
100	0.6	1.15	microgels

mL), microspheres with average diameters of 2.3 μm and a lower PDI of 1.06 could be formed.

Intermediate morphologies appear at the edges of the microsphere solvent window. At a composition of 25% xylenes small microspheres (1.2 μm) were generated with a significant proportion of interconnected particles of the same size. With 65% xylenes microspheres were formed. However, the particles were not discrete and again appeared to be interconnected.[34]

(ii) Influence of the Monomer Ratio. The synthesis of crosslinked polystyrene particles has been shown to be affected by the proportion of DVB in the reaction mixture.[27] For relatively low DVB concentrations (less than 10%), soluble polymeric material is generated. However, by simply increasing the amount of DVB in the reaction mixture, several other morphological transitions were observed to, for example, space-filling gels, microspheres, and coagula.

To probe the effects of the cross-link ratio on the formation of autostabilized PFSMSs, the relative amount of the spirocyclic monomer **4** was increased from 0 to 100%, producing a wide range of observed morphologies (Table 2).[34]

(a) Low Cross-Link Ratios (0−20% Monomer 4). With small amounts of the spirocyclic monomer **4** added to the reaction ill-defined polymer particles were formed. Reactions involving no added monomer **4** produced a polymeric precipitate with a number average molecular weight of 35,100 and a polydispersity of 1.8 relative to polystyrene standards. By increasing the amount of spirocyclic monomer **4** to 20%, highly swollen polymeric microgels were formed which collapsed upon washing with methanol, producing interconnected particles with average diameters of ca. 2.8 μm.[34] With such a low cross-link density, desolvation and subsequent hardening of the particles do not occur during the course of the reaction, and upon workup with methanol the particles cannot maintain their spherical shape and appear attached.

(b) High Cross-Link Ratios (80−100% Monomer 4). Above 65% added monomer **4**, highly irregular particles were formed which appeared to become more interconnected with increasing amounts of **4**. Such an interconnected network of particles in this case may be due to an increased surface reactivity when a high concentration of difunctional monomer is present and particle fusion becomes more likely. Furthermore, the size of these polymeric nodules was much smaller than that previously encountered at this solvent composition, which may be due to an increased cross-link density of the particles. Higher cross-linking density would also cause a reduction in the solvent-swollen gel layer, which is necessary to maintain colloidal stability of the particles.

Table 2. Effect of Monomer Ratio on the Observed Particle Morphology

amt of **4** (mol %)	av diam (μm)	PDI	morphology
0			soluble polymer
20	2.8	1.2	interconnected particles
40	2.2	1.2	interconnected spheres
50	2.6	1.1	spheres
60	1.5	1.1	spheres
80	1.0	1.2	interconnected particles
100	1.0	1.2	interconnected particles

Table 3. Effect of Catalyst Concentration on the Observed Particle Morphology

amt of catalyst (mol %)	av diam (μm)	PDI	morphology
0.3	2.2	1.14	spheres
0.6	2.5	1.17	spheres
1.2	2.6	1.10	spheres
1.8	3.1	1.12	spheres (bimodal)
	0.9	1.47	spheres (bimodal)

(c) Intermediate Cross-Link Ratios (40−60% Monomer 4). With moderate amounts of the spirocyclic ferrocenophane **4,** discrete polymer microspheres were formed with sizes ranging from 1.5 to 2.6 μm and PDI < 1.2 (see Table 2). For samples with greater compositions of monomer **4**, the particles were generally smaller in size, consistent with an increase in the cross-link density. Under these conditions, the particles presumably have the necessary degree of cross-linking to expel solvent from the core, forming nucleation sites for further growth, and maintain this solvent-swollen shell, which captures reactive oligomers in solution.

(iii) Influence of Precatalyst Concentration. The amount of precatalyst added to the reaction medium may affect the rate of the polymerization, and ultimately influence the resulting particle morphology. The mechanism of the transition-metal-mediated ROP of [1]silaferrocenophanes is not fully understood but appears to involve colloidal platinum as the active catalyst.[29] As particle nucleation is essential to control particle growth, higher concentrations of the precatalyst may result in an increase in the number of sites available for particle nucleation and growth.[34]

The amount of precatalyst was varied from 0.3 to 1.8 mol % in the reaction vessels, forming spherical particles ranging in size from 2.2 to 3.1 μm (see Table 3). With small amounts of catalyst (0.3 and 0.6 mol %) the particles possessed average diameters of 2.2 μm (PDI = 1.14) and 2.5 μm (PDI = 1.17), respectively. At relatively high concentrations of catalyst (1.8 mol %), a bimodal particle size distribution was observed which appears to be the result of secondary nucleation at later stages in the reaction.[34]

The most well-defined particles were formed with 1.2 mol % added precatalyst, which produced particles of relatively low PDI (<1.10) with average diameters of 2.6 μm. Secondary nucleation is avoided while a competitive polymerization rate is maintained to allow for the formation of autostabilized microspheres of uniform size and surface topology.

(iv) Evolution of Particle Morphology. To investigate the growth rate of PFSMSs, a study of the resulting particle morphology over time was conducted. Preliminary studies showed that the majority of particle nucleation and growth occurs in the first 4−5 h of the reaction. Monitoring the morphologies produced during these initial stages was expected to provide key insight into the particle nucleation and growth mechanism.

(a) Newly Formed Particles. Early in the reaction (<0.5 h), soluble, weakly cross-linked microgels are observed due to a relatively low degree of cross-linking (see Figure 4A). Such structures are believed to serve as nucleation sites for future growth of polymer microspheres and collapse upon removal from the reaction medium. As the reaction continued, a remarkable morphology was observed at 1.0 h, consisting of an array of smooth polymer nodules, interconnected by narrow polymeric "bridges" (see Figure 4B). A smooth surface topology is due to the collapse of weakly cross-linked, newly formed polymer particles during workup in methanol. The particles remain connected by polymeric material at the points of contact between nodules. This confirmed that, at this stage of the reaction, the PFS was only weakly cross-linked and remained highly swollen in the reaction medium, allowing for further surface reactions.[34]

At ca. 1.5 h a new surface morphology was observed with the appearance of discrete particles with a high surface roughness (Figure 4C). These particles appear elongated following sample workup with a significant decrease in the degree of interconnections between particles. Such rough particle surfaces have been observed for polystyrene microspheres formed under poor solvency conditions. This highly variable surface topology is believed to be the result of a lightly cross-linked polymer gel layer which is covalently bonded to the surface of the particles. Therefore, the newly formed PFSMSs appear to be more highly cross-linked and remain as discrete particles when placed in a non-solvent during washing. However, as their surface is only moderately cross-linked a nonuniform collapse of the solvent-swollen outer gel layer produces a rough surface topology. Newly formed particles appear as interconnected particles with smooth surfaces due to a reduced cross-link density.

(b) Particle Growth. By 2 h, the majority of the particles have high surface roughness, and relatively high polydispersity (≤3.0, Figure 4D). The particles remain elongated due to inhomogeneous collapse of the polymer networks. Any residual polymer "bridges" appear only as small nodules on the surface of a small number of particles. By this stage of the reaction new particle formation has been minimized.

During the next 2 h (Figure 4E−H) the particles were found to decrease in surface roughness and form spherical particles with improved polydispersity indices (see Table 4). Such effects are found for highly cross-linked particles that retain their shape during workup in a non-solvent. By 4.5 h (Figure 4I), the surface morphology of all particles appears to be smooth, with an average diameter of 2.1 μm (PDI of 1.14). Similar morphologies were found for polystyrene microspheres for which particle growth is believed to occur by a homogeneous precipitation polymerization (Scheme 2).

(c) Proposed Mechanism. The formation of PFSMSs appears to follow a nucleation and growth mechanism similar to that proposed for their polystyrene analogues (Scheme 2) despite inherent differences in their polymerization methods (i.e., transition-metal-catalyzed ROP versus free radical polymerization). Particle nucleation appears to occur within the first 1−2 h of the reaction involving the desolvation of isolated microgels within the reaction mixture. Particle growth occurs over the next few hours as the solvent-swollen outer gel layer binds to the reactive monomer and oligomeric species present in solution. As with polystyrene microspheres, the particles become more highly cross-linked during the course of the reaction, and are able to maintain a smooth spherical shape when placed in a non-solvent such as methanol.

Interestingly, a significant difference between the present system and the case of crosslinked polystyrene microspheres is found as the particle size of PFSMSs is observed to *increase* with addition of a more favorable solvent such as xylenes. Both poly(styrene-*co*-divinylbenzene) spheres[27] and poly(maleic anhydride-*alt*-divinylbenzene) spheres[35] showed a *decrease* in particle diameter with increasing solvency of the polymerization mixture. In the case of the polystyrene microspheres, this solvent effect was attributed to better surface solvation, stabilizing the growing particles against oligomer binding, and hence leading to more and smaller particles surviving to the final stage. In the case of PFSMSs, although we have no convincing explanation for the opposite solvent effect observed, it may be a consequence of a higher degree of *overall* swelling of the growing microspheres, enabling them to better capture oligomers from the solution.

Properties of PFSMSs. (i) Oxidation of PFSMSs and Their Subsequent Electrostatic Self-Assembly. On the basis of previous work with polyferrocenylsilanes **2**,[10,15] chemical oxidation of the PFSMSs should be possible, thereby resulting in the formation of a positively charged outer surface. These positively charged particles would be expected to electrostatically self-assemble with oppositely charged particles such as negatively charged silica microspheres. When an orange suspension of PFSMSs **(**ca. 2.6 μm in diameter**)** in methanol was added to a white suspension of smaller silica microspheres (ca. 0.4 μm in diameter) in water, a yellow, opaque suspension was obtained. Treatment of this mixture with excess methanolic I_2 resulted in an immediate color change to light green, consistent with oxidation of the iron centers in the PFSMSs to yield the corresponding oxidized species, OPFSMSs.[36] Samples analyzed by SEM were prepared by deposition onto a Si wafer, followed by solvent evaporation. The presence of composite superstructures in which the larger OPFSMSs were surrounded by the smaller, negatively charged spherical silica particles was observed (Figure 5A).[37] Given that the silica particles appeared to have surrounded the whole of the OPFSMSs, these satellite structures are a result of an electrostatically driven self-assembly of silica spheres onto OPFSMSs and are not due to simple

(35) Frank, R. S.; Downey, J. S.; Stöver, H. D. H. *J. Polym. Sci., Part A.: Polym. Chem.* **1998**, *36*, 2223.

(36) For PFSs, metal−metal interactions along the polymer backbone lead to the presence of two reversible oxidation waves (redox coupling, $\Delta E \approx$ 250 mV) as illustrated by cyclic voltammetry studies. Thus, with a relatively weak oxidant such as I_2, the redox potential lies very close to that of the first oxidation wave of the polymer. A maximum of 1/2 of the ferrocene sites can react to form ferrocenium centers. However, with relatively strong oxidants such as $[N(C_6H_4Br\text{-}p)_3][SbCl_6]$ or $[N(C_6H_4Br\text{-}p)_3][PF_6]$ all of the ferrocene moieties can react. See for example: (a) Rulkens, R.; Resendes, R.; Verma, A.; Manners, I.; Murti, K.; Fossum, E.; Miller, P.; Matyjaszewski, K. *Macromolecules* **1997**, *30*, 8165. (b) Connelly, N. G.; Geiger, W. E. *Chem. Rev.* **1996**, *96*, 877. (c) See ref 15.

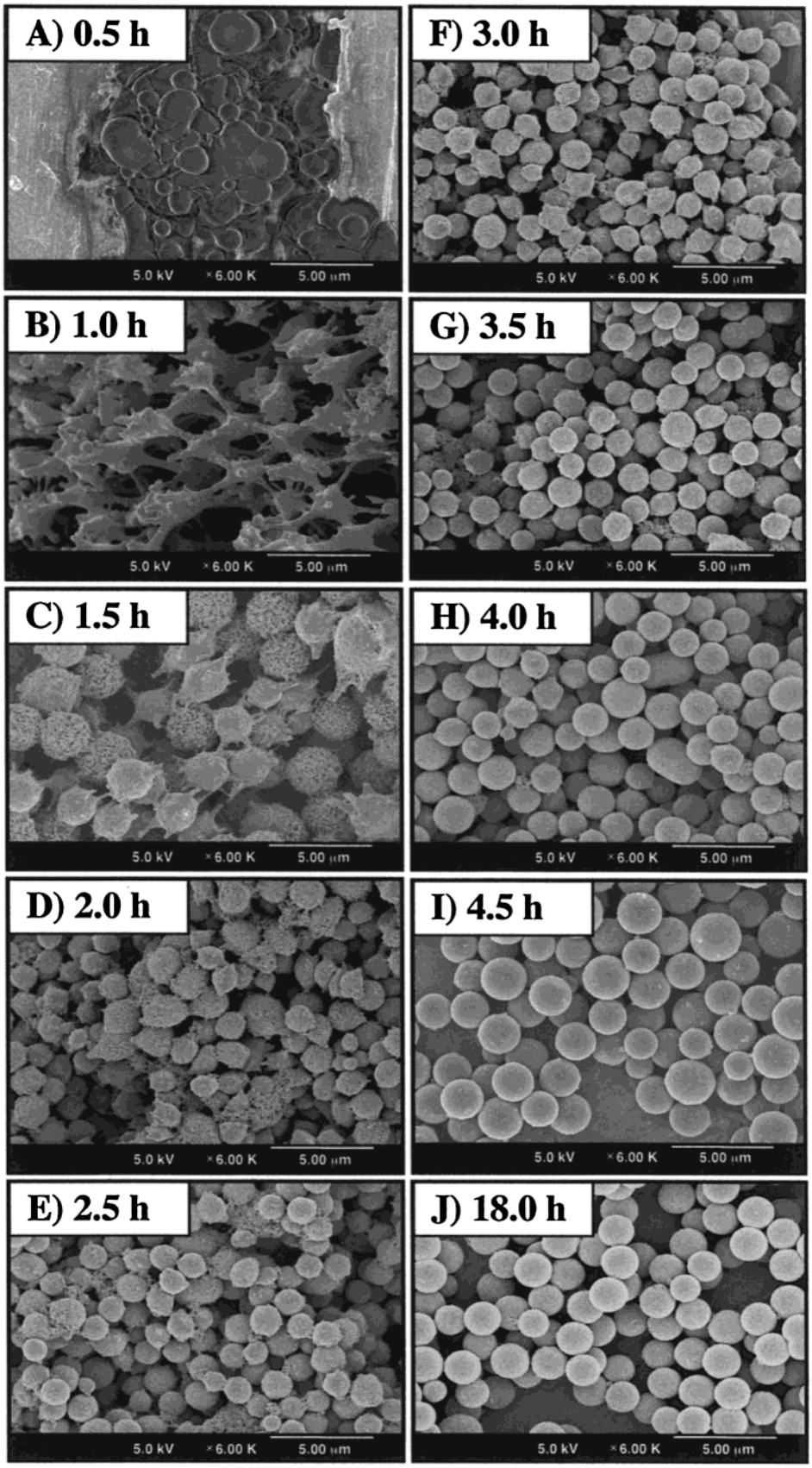

Figure 4. Particle morphology observed during the course of the precipitation polymerization reaction of PFSMSs.

evaporative deposition. Also observed in the sample were areas in which the OPFSMS composite particles were circumscribed by regions of silica spheres (Figure 5B); this phenomenon may be the result of evaporation-induced self-assembly.

Table 4. Effect of Reaction Time on Particle Size

time (h)	av diam (μm)	PDI	time (h)	av diam (μm)	PDI
2.5	1.5	1.20	4.0	1.7	1.12
3.0	1.5	1.14	4.5	2.1	1.14
3.5	1.5	1.14	18.0	2.6	1.10

As silica particles fuse at ca. 800 °C and polyferrocenylsilanes form magnetic ceramic materials above 600 °C, the silica−polyferrocenylsilane composite microspheres represent intriguing precursors to core−shell ceramic composites. Also, by matching the size of the silica particles to that of the polyferrocenylsilane microspheres, it may be possible to form AB and AB_2 lattices similar to those observed for colloidal Au and Ag particles.[38]

The accessibility of the ferrocene sites within the PFSMSs is of considerable interest as this would govern the redox chemistry of these particles. Gas adsorption measurements show these particles to have a low surface area (4 m^2/g) indicative of a material of low porosity. Thus, only the surface of the particles can be expected to be available for chemical reactions in the solid state. Oxidation with I_2 vapor allows a convenient probe to study the porosity of the polymer particles by TEM cross-sectional analysis.[36] No I_2 was observed to penetrate to the interior of the particles, and only the surface of the particles appeared to be stained with the chemical oxidant. The existence of iodine on the surface of the oxidized PFSMSs was confirmed by XPS analysis.[34]

To further probe the oxidation of these spheres in solution, a strong one-electron oxidant, $[N(C_6H_4Br\text{-}p)_3][SbCl_6]$, was used, allowing for a more controlled oxidation of the microspheres in acetonitrile. The oxidation of the microspheres was confirmed by UV−vis/near-IR spectroscopy (oxidation and reduction) using excess oxidant followed by chemical reduction of the particles with hydrazine in methanol. Oxidation of the iron sites was confirmed by the appearance of an intervalence charge-transfer band (800−1800 nm) and a ligand to metal transfer band centered at 640 nm in the UV−vis /near-IR spectrum of the oxidized microspheres.[34] Reduction with hydrazine in methanol returned the OPFSMSs to their initial, neutral (fully reduced) state.

(ii) Controlled Oxidation of PFSMSs by $[N(C_6H_4Br\text{-}p)_3][PF_6]$. A Redox Titration. To determine the accessibility of the ferrocene sites in solution and to test the charge tunability of the PFSMSs, a redox titration was performed in acetonitrile. To eliminate any possibility of small amounts of side reactions with the $[SbCl_6]^-$ anion, the $[N(C_6H_4Br\text{-}p)_3][PF_6]$ salt was utilized.[36] Furthermore, as the end point of the titration was difficult to observe visually, the conductivity of the solution was used to monitor the redox reaction. Free ions have a significantly higher mobility in solution than when tightly associated with a charged surface.[39] Consequently, we anticipated that, as the added $[N(C_6H_4Br\text{-}p)_3][PF_6]$ salt reacts with the ferrocene centers present on the PFSMS surface, the resulting conductivity increase would be relatively small. Once all of the accessible ferrocene moieties had reacted, any additional salt would be expected to contribute free ions to the solution, and as a result, the conductivity should be seen to increase dramatically.

As expected, the conductivity of the solution increased linearly when controlled amounts of a 9.2 mM solution of $[N(C_6H_4Br\text{-}p)_3][PF_6]$ in acetonitrile were added to a blank solution cell (i.e., without added PFSMSs). Such an effect is due to an increased concentration of free ions present in the solution upon addition of the oxidant. In the presence of PFSMSs (2.6 μm diameter, PDI = 1.10), however, the conductivity increase is modified. Only after ca. 2.6 mL of oxidant addition does the conductivity response match that of free ions (see Figure 6). The end point corresponded to oxidation of 32% of the ferrocene centers present in the PFSMSs or the outer 0.15 μm of the particle. Thus, the ferrocene sites appear to be more accessible in solution than in the solid state. In solution, the presence of charged ferrocenium centers on the PFSMS surface may lead to a preferential swelling of the polymer network in acetonitrile and thus increase the availability of ferrocene sites for further reaction.[40]

(iii) Pyrolysis of Microspheres to Spherical Magnetic Ceramic Particles. The development of magnetic particles is of intense interest for theoretical studies[41] and potential use in a range of microsystems and magnetic imaging applications.[42] Well-defined spherical magnetic particles are particularly attractive for many studies as these species can self-assemble into well-ordered thin films possessing a high density of regularly spaced magnetic domains.[43] Recently, magnetite (Fe_3O_4) was deposited onto polystyrene latex spheres (ca. 600 nm) which were surface modified with various polyelectrolytes.[8a,b] This resulted in magnetic composite particles, which can self-assemble and align under the influence of an external magnetic field.

The cross-linked PFSMSs were considered as potential precursors to spherical magnetic ceramic (SMC) particles.[44] To study the morphology of the resulting ceramic particles, 2-D arrays of PFSMSs (2.6 μm in diameter with a PDI of 1.06) were prepared and then pyrolyzed (under N_2) from 600 to 1000 °C (Table 5). SEM analysis of the resulting materials formed at 600 and 900 °C confirmed the formation of spherical ceramic

(37) Using a stronger chemical oxidant such as $[N(C_6H_4Br\text{-}p)_3][SbCl_6]$ results in a greater surface coverage of the OPFSMSs with the negatively charged silica spheres. Without chemical treatment with I_2, PFSMSs and the colloidal silica particles settle independently, without the formation of composite particles. Investigations into the electrostatic interactions present in these composite materials are currently under way in our laboratories.

(38) (a) Kiely, C. J.; Fink, J.; Zheng, J. G.; Brust, M.; Bethell, D.; Schiffrin, D. J. *Adv. Mater.* **2000**, *12*, 640. (b) Galow, T. H.; Boal, A. K.; Rotello, V. M. *Adv. Mater.* **2000**, *12*, 576.

(39) Shaw, D. T. *Introduction to Colloid and Interface Science*, 4th ed.; Butterworth Hienmann: Oxford, 1992.

(40) Ferrocene and ferrocenium (fcH_2^+) display markedly different solubility characteristics. For example, $[fcH_2][PF_6]$ is soluble in water, while ferrocene is completely insoluble. Therefore, polar solvents (such as acetonitrile) would be expected to swell the oxidized particles to a greater extent relative to the untreated PFSMSs.

(41) (a) Takahashi, T.; Dimitrov, A. S.; Nagayama, K. *J. Phys. Chem.* **1996**, *100*, 3157. (b) Dimitrov, A. S.; Takahashi, T.; Furusawa, K.; Nagayama, K. *J. Phys. Chem.* **1996**, *100*, 3163. (c) Golosovsky, M.; Saado, Y.; Davidov, D. *Appl. Phys. Lett.* **1999**, *75*, 4168.

(42) (a) Deng, T.; Whitesides, G. M.; Radhakrishnan, M.; Zabow, G.; Prentiss, M. *Appl. Phys. Lett.* **2001**, *78*, 1775. (b) Schueller, O. J. A.; Brittain, S. T.; Marzolin, C.; Whitesides, G. M. *Chem. Mater.* **1997**, *9*, 1399. (c) Raj, K.; Moskowitz, R. *J. Magn. Magn. Mater.* **1990**, *85*, 233.

(43) For some recent examples of magnetic nanoparticle assembly, see: (a) Petit, C.; Taleb, A.; Pileni, M.-P. *Adv. Mater.* **1998**, *10*, 259. (b) Ngo, A.-T.; Pileni, M.-P. *Adv. Mater.* **2000**, *12*, 276. (c) Stamm, C.; Marty, F.; Vaterlaus, A.; Weich, V.; Egger, S.; Maier, U.; Ramsperger, U.; Fuhrmann, H.; Pescia, D. *Science* **1998**, *282*, 449. (d) Sun, S.; Murray, C. B.; Weller, D.; Folks, L.; Moser, A. *Science* **2000**, *287*, 1989.

(44) For work on polymeric ceramic precursors, see: (a) Baldus, H.-P.; Jansen, M. *Angew. Chem., Int. Ed. Engl.* **1997**, *36*, 328. (b) Segal, D. *J. Mater. Chem.* **1997**, *7*, 1297. (c) Bill, J.; Aldinger, F. *Adv. Mater.* **1995**, *7*, 775. (d) Laine, R. M.; Babonneau, F. *Chem. Mater.* **1993**, *5*, 260. (e) Liu, Q.; Shi, W.; Babonneau, F.; Interrante, L. V. *Chem. Mater.* **1997**, *9*, 2434.

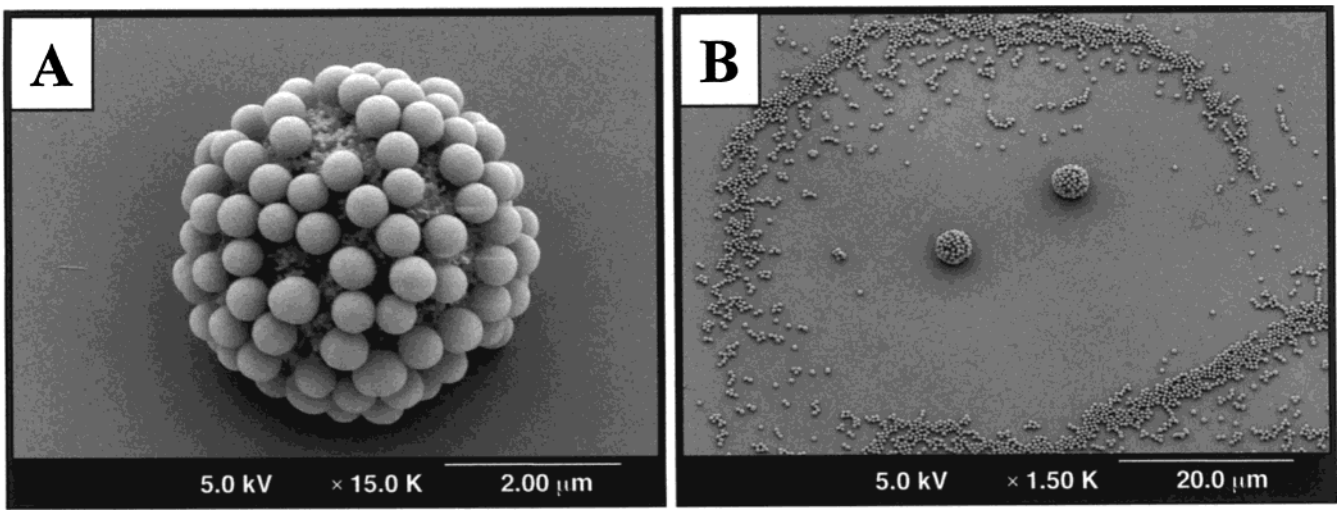

Figure 5. SEM micrographs of (A) negatively charged silica microspheres electrostatically bound to the surface of OPFSMSs and (B) surface patterns of core-corona OPFSMS−silica assemblies circumscribed by regions of silica spheres.

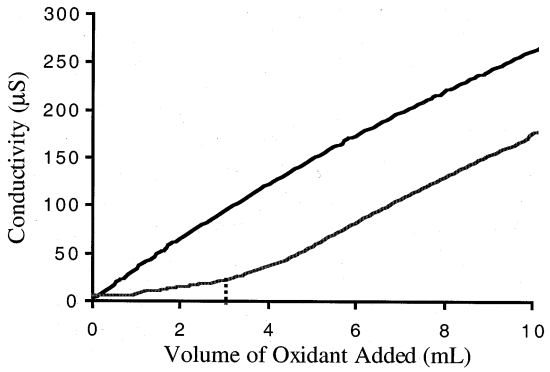

Figure 6. Redox titration of PFSMSs. The upper line shows the conductivity of the solution with controlled amounts of a 9.2 mM solution of $[N(C_6H_4\text{-}Br\text{-}p)_3][PCl_6]$ in acetonitrile added. The lower line shows the conductivity response of the solution with 18.5 mg of PFSMSs present in the reaction mixture.

Table 5. Polyferrocenylsilane Ceramic Microspheres

temp (°C)	av diam (μm)	PDI	ceramic yield (%)
600	1.9	1.08	85.2
700	1.7	1.07	84.7
800	2.1	1.13	84.0
900	1.8	1.08	72.7
1000	2.2	1.11	77.8

particles with average particle diameters of 1.9 μm (PDI of 1.08) and 1.8 μm (PDI of 1.08), respectively (Figure 7A,B).

Thin cross-sections of the ceramic particles formed at 600 and 900 °C were studied using TEM. The ceramic particles formed at lower temperature appear amorphous and have a near-homogeneous texture throughout the entire sphere. In marked contrast, the spherical ceramics formed at 900 °C clearly show the presence of α-Fe nanoparticles with dimensions of 10−100 nm dispersed throughout the material (Figure 7C,D).

The ceramic particles formed at 600 °C were amorphous by PXRD. At 700 °C a small amount of α-Fe particles was detected with a broad peak centered near $2\theta = 45°$, $d = 2.03$ Å attributed to the 110 reflection of crystalline α-Fe. At higher temperatures, this peak grows in intensity owing to the presence of larger α-Fe particles. Low-intensity broad bands assigned to the 002 reflection of graphite centered at $2\theta = 26°$, $d = 3.38$ Å and the 110 reflection of γ-Fe centered at $2\theta = 43$, $d = 2.08$ Å became observable at temperatures over 800 °C. Further analysis of the 110 reflection of α-Fe using the Scherrer equation[45] estimated the average particle sizes of the α-Fe clusters in the ceramic spheres to be ca. 4 nm at 700 °C, with larger diameter particles formed at 800 °C (17 nm) and 900 °C (22 nm). These values are similar to the size of crystallites present in the bulk ceramic derived from **5** ($x = y = 0$) pyrolyzed over a similar temperature range.[21] The composition of the resulting ceramic material varied with respect to the relative amounts of the of α- and γ- forms of Fe crystallites as well as the amount of Fe_3O_4 observed. Such a range of ceramic compositions may be the result of the high surface area of the polymer particles in comparison with bulk samples.[21]

The ceramic particles derived from PFSMSs pyrolyzed above 700 °C are magnetic, as shown by their attraction to a bar magnet. Detailed investigation of the magnetic properties for ceramic microspheres formed at 700 and 900 °C was undertaken using SQUID magnetometry.

ZFC DC-susceptibility data revealed a "blocking temperature" T_b at 60 K for ceramics formed at 700 °C, defined as the temperature cusp in the ZFC susceptibility curve. This would indicate that the sample is a superparamagnet above 60 K. However, the isothermal magnetization versus applied field data (Figure 8) were found to show non-superimposable hysteresis loops at both 5 and 250 K for ceramics formed at 700 °C. This behavior is due to a distribution in the sizes of the α-Fe crystallites within the sample. Some of the particles are multidomain particles (i.e., larger than the Weiss domain, 14 nm) and behave ferromagnetically above the blocking temperature (60 K). Most of the crystallites in the sample are near or below this size and only behave ferromagnetically below the blocking temperature. These SMCs possess a coercive field of 0.015 T at 5 K and 0.001 T at 250 K with saturation magnetizations (M_s) of 9 emu/g.

No apparent blocking temperature was found for ceramics formed at 900 °C (Figure 8B). For ceramics formed at 900 °C, the α-Fe crystallites display ferromagnetic properties at room

(45) Cullity, B. D. *Elements of X-ray Diffraction*; Addison-Wesley Publishing Co. Inc.: Reading, MA, 1978.

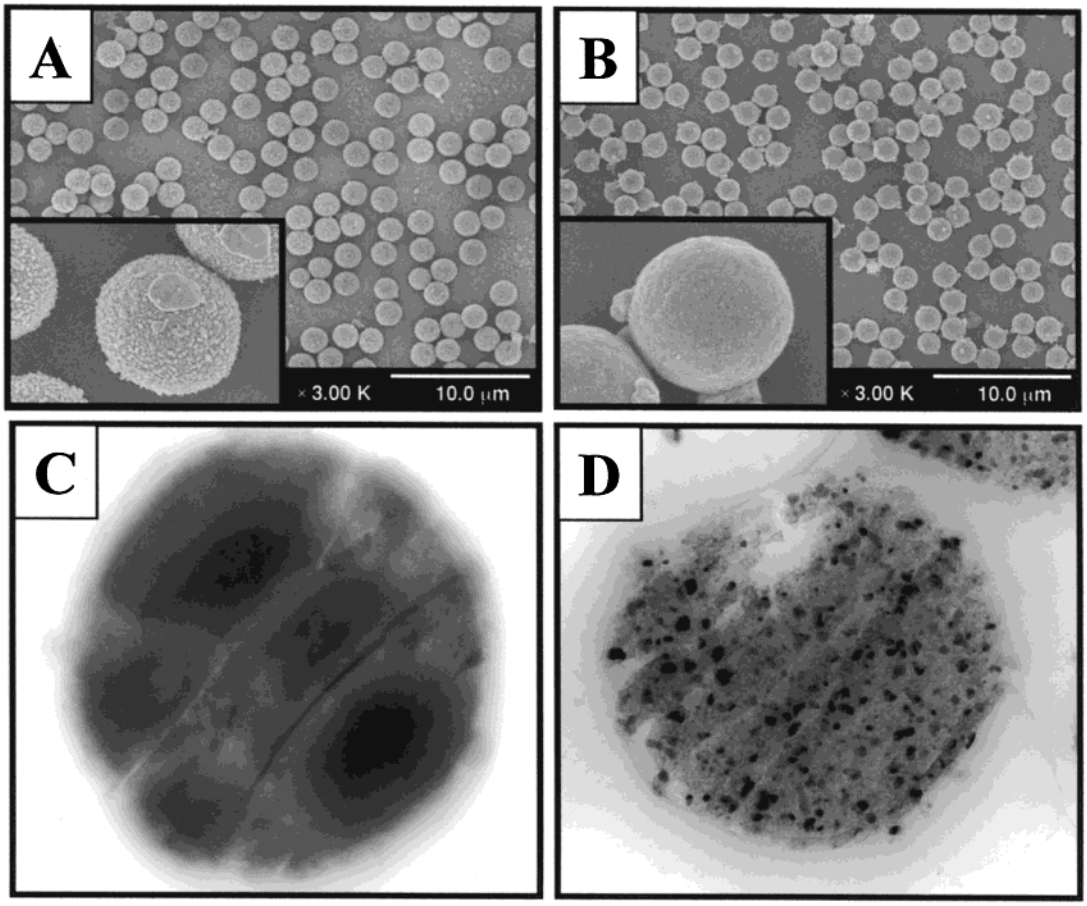

Figure 7. SEM and thin-section TEM micrographs of ceramic particles obtained from pyrolysis of PFSMSs under a nitrogen atmosphere for (A, C) 2 h at 600 °C and (B, D) 2 h at 900 °C. The fractures present in the cross-sections are a result of the microsectioning.

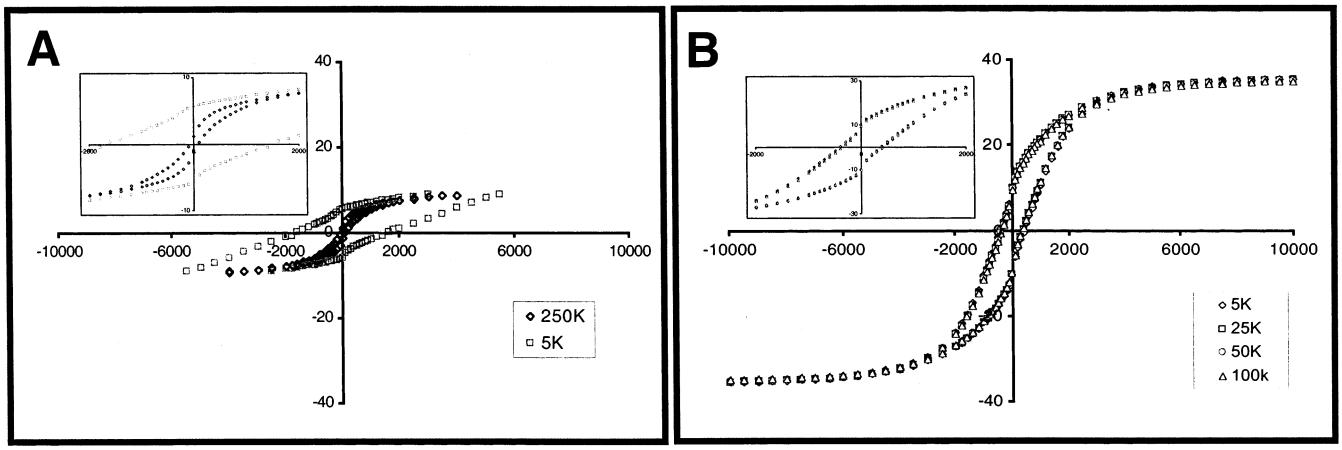

Figure 8. Magnetic measurements of SMCs obtained from pyrolysis of PFSMSs at (A) 700 °C showing non-superimposable hysteresis loops recorded at 5 and 250 K and (B) 900 °C showing superimposable magnetization curves recorded at 5, 25, 50, and 100 K. Insets show expansions of magnetization curves.

temperature with overlapping hysteresis loops at all temperatures measured. Such behavior is indicative of the presence of multidomain, ferromagnetic particles.[46] These SMCs possess a coercive field of 0.04 T, a saturation magnetization of 35 emu/g, and a remanence ratio of 0.28, which is characteristic of a soft ferromagnet such as α-Fe.

Such tunable magnetic behavior has been shown for the bulk ceramic material derived from **5** ($x = y = 0$)[21] for which the magnetic properties are tuned from superparamagnetic to ferromagnetic depending on the pyrolysis conditions. At higher temperatures ferromagnetic particles are formed, while smaller superparamagnetic particles are formed at lower temperatures.

As a result of the magnetic properties associated with the SMC particles, their assembly into well-ordered arrays by application of an external magnetic field was explored.[41,47] It was observed that diffuse monolayers of SMC particles formed at an air−water interface can be affected by the application of a strong magnetic field (Figure 9A). For instance, long strings

(46) Leslie-Pelecky, D. L.; Rieke, R. D. *Chem. Mater.* **1996**, *8*, 1770 and references therein.

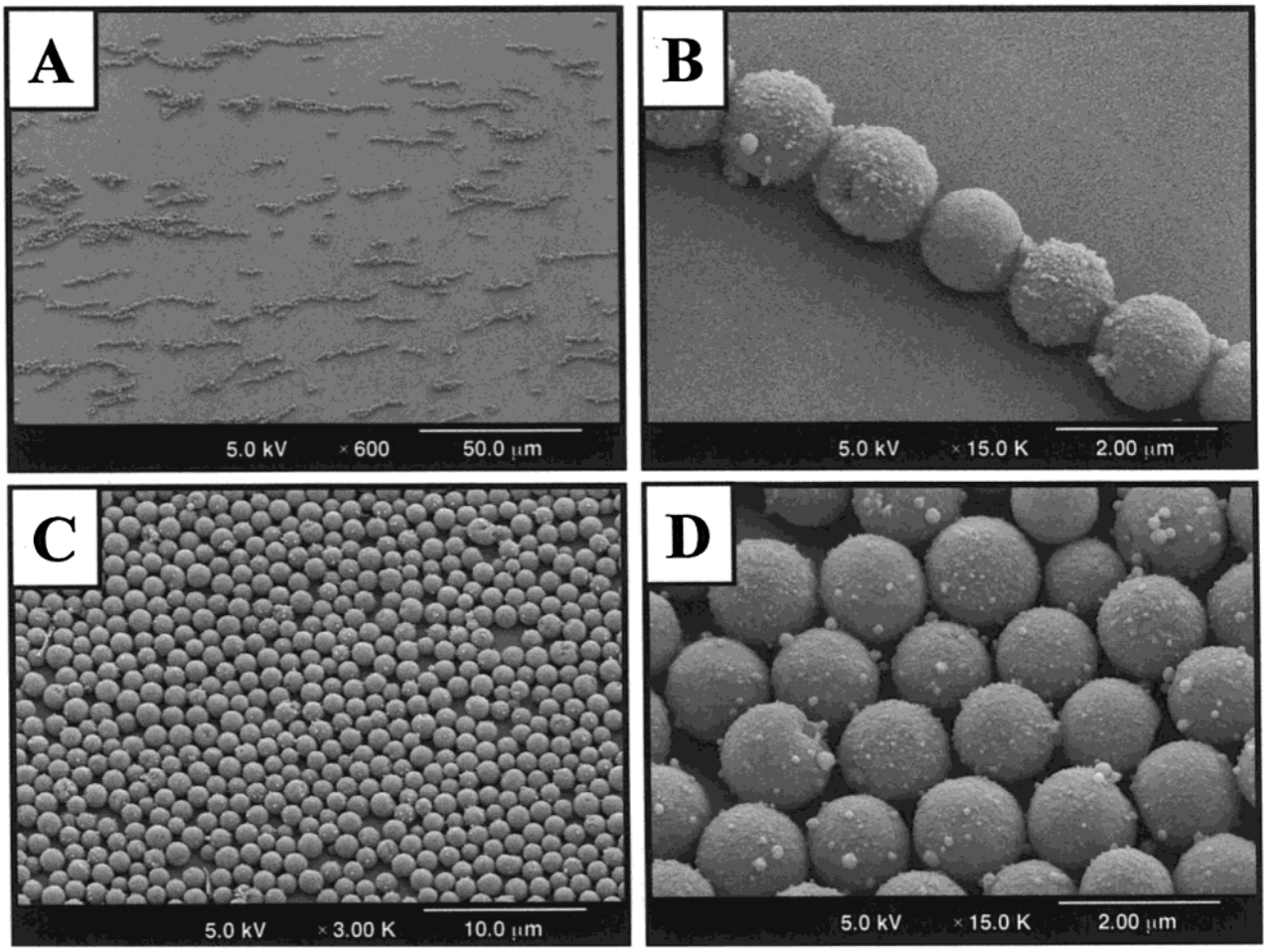

Figure 9. SMCs obtained from pyrolysis of PFSMSs at 900 °C displaying magnetic ordering in an external magnetic field. SEM showing (A, B) aligned strands and (C, D) a tightly packed monolayer with small regions of close-packed ceramic microspheres.

of SMC particles are formed due to significant interactions with the magnetic field lines of a single SmCo rare-earth-metal magnet (Figure 9B). In addition, it is possible to form close-packed 2-D arrays between the poles of two SmCo magnets. In this instance, the magnetic spheres are forced together into a tightly packed array at the air−water interface and highly ordered sections within the 2-D array are clearly evident (Figure 9C,D). The adjustment of the magnitude and direction of the applied magnetic field may further allow for tuning of the interparticle spacing. Such interactions may ultimately be useful in the formation of tunable photonic band gap materials.[5,48,49]

Summary

We report the first synthesis of microspheres comprised of polyferrocenylsilane, a metallopolymer, by a precipitation polymerization methodology. Upon oxidation, PFSMSs undergo electrostatic self-assembly with silica spheres to form core−shell composite particles. PFSMSs possess a relatively low porosity in the solid state. However, ca. 1/3 of the ferrocene moieties are available for solution redox chemistry. Furthermore, by varying the amount of oxidant used, the degree of oxidation of PFSMSs, and therefore the charge, can be controlled. Upon thermal treatment, the PFSMSs are transformed with shape retention into ceramic microspheres containing α-Fe nanoclusters embedded within a silicon carbide−carbon matrix. Variation of the pyrolysis conditions leads to ceramics with tunable magnetic properties from the superparamagnetic state to the ferromagnetic state, which can be formed into organized arrays in the presence of an external applied magnetic field.

Precipitation polymerization methods are able to produce crosslinked polystyrene microspheres with a PDI near 1.01. Future studies of PFSMSs will explore the use of more well-defined catalyst systems, different solvents, and other difunctional [1]silaferrocenophanes with the aim of accessing even more well-defined particles (PDI < 1.06). Such microspheres with tailorable redox, semiconductive, and magnetic properties may find use in controlled crystallization applications, tunable photonic devices, and the formation of a variety of microsystems.

Acknowledgment. We thank Dr. Nicholas Burke for conductivity measurements, Randy Frank, Jeff Downey, and Guodong Zheng for helpful discussions, Marc Mamak for PXRD, and Dr. San-Ming Yang and André Arsenault for providing silica microspheres and for helpful discussions. We also thank Cindy Huctwith, Brad Kobe, and the staff at Surface Science Western for SEM and optical microscopy as well as

(47) (a) Grzybowski, B. A.; Stone, H. A.; Whitesides, G. M. *Nature* **2000**, *405*, 1033. (b) Grzybowski, B. A.; Jiang, X.; Stone, H. A.; Whitesides, G. M. *Phys. Rev. E* **2001**, *64*, 011603.
(48) (a) Gates, B.; Xia, Y. *Adv. Mater.* **2001**, *13*, 1605. (b) Yi, G.-R.; Moon, J. H.; Yang, S.-M. *Adv. Mater.* **2001**, *13*, 1185.
(49) Xu, X.; Friedman, G.; Humfeld, K. D.; Majetich, S. A.; Asher, S. A. *Adv. Mater.* **2001**, *13*, 1681.

Professor K. Balmain and Gerald Dubois for the use of SmCo magnets and for helpful discussions. K.K. and R.R. are grateful to NSERC and A.C. and A.B. are grateful to the University of Toronto for postgraduate scholarships. We thank the Canadian Government for a Canada Research Chair in Materials Chemistry (2001−2008, G.A.O.) and in Inorganic and Polymer Chemistry (2001−2008, I.M.). In addition I.M. thanks NSERC for an E.W.R. Steacie Fellowship (1997−99), the University of Toronto for a McLean Fellowship (1997−2002), and the Ontario Government for a PREA Award (1999−2004) for the duration of the work described.

Supporting Information Available: Experimental Section, spectral data for PFSMSs (solid-state NMR, reflectance UV−vis/near-IR, XPS, and PXRD data), and SEM and TEM images for the experiments outlined in the text (PDF). This material is available free of charge via the Internet at http://pubs.acs.org.

JA0202053